Electric Field Distribution
in a Reverse-Biased *p*-*n* Junction

Kirk T. McDonald

Joseph Henry Laboratories, Princeton University, Princeton, NJ 08544

(November 17, 2012; updated September 13, 2015)

1   Problem

This problem is motivated by the use of crystals as detectors of energetic charged particles that pass completely through the crystal, leaving a trail of electron-ion pairs. Although the crystals are nominally insulators, the electrons so liberated are in the conduction band and can be separated from the ion by a DC electric field, resulting in a signal pulse on the electrodes plated onto opposite faces of the crystal.[1,2,3] However, recombination of the drifting electrons at impurity sites is an issue, and it was eventually realized that the high purities of germanium and silicon required for successful transistors are also good for crystalline particle detectors.[4] In addition, *p*-*n* diode junctions proved to be suitable for particle detectors [10].

A typical silicon *p*-*n* junction is illustrated below, in which a potential difference $\Delta V \approx$ 0.8 V develops across the junction in the absence of an external bias voltage,[5] due to the layers of (space) charge, a few μm thick. The *p*-side of the junction is doped with a bulk number density N_p (or N_a) of atoms (such as boron) with 3 valence electrons (compared to 4 for Si), called acceptors in that these atoms can accept electrons from neighboring atoms, the motion of which electrons in one direction corresponds to a current of (electrically positive) holes in the other. The *n*-side is doped with number density N_n (or N_d) of atoms with 5 valence electrons (such as phosphorus), called donors.[6] A electron current can flow from the *n*-side to the *p*-side only if an external (forward) bias voltage $V_p - V_n > \Delta V$ is applied, and no (significant) electron current flows from the *p*-side to the *n*-side for any applied voltage less than this. The *p*-*n* junction acts as a diode/rectifier.

Doped silicon has "free" charge carriers, predominantly holes in *p*-doping and predominantly electrons in *n*-doping. As such, the can be no electric field inside the doped silicon

---

[1]Crystals with metallic electrodes are metal-semiconductor junctions, first investigated by Braun in 1874 [1]. Popular interest in such junctions arose in 1906 following the discovery that a metal-carborundum junction rectifier could be used to detect radio signals in what is now call a crystal radio set [2, 3].

[2]The metal-semiconductor junctions are often called Schottky (barrier) diodes [4], although the full theory of their operation is due to Bethe [5].

[3]The earliest attempt at detection of an electrical signal due to (α) particles in a crystal appears to have been in 1906 by a student of Röntgen [6]. The first successful detection may have been by van Heerden in 1946 [7]. Some of the rapid development thereafter in the late 1940's can be traced in [8].

[4]Not all energy deposited in the crystal by energetic charged particles is goes into creation of electron-ion pairs. Some energy goes into the emission of optical photons, which can be detected externally if the crystal is transparent. The development of purer material for the semiconductor industry also led to new developments in crystal scintillators [9].

[5]ΔV is necessarily less than the gap of $\approx$ 1.17 V (at room temperature) between the valence and conduction bands in Si. Thermal excitations result in a nonzero charge densities on either side of the junction, whose associated electric field leads to the potential difference ΔV, as first well-discussed by Shockley [11].

[6]Doped silicon is electrically neutral when subject to zero external potential difference.

under reverse bias, unless all of the "free" charge carriers have been removed, and the silicon is said to be depleted.
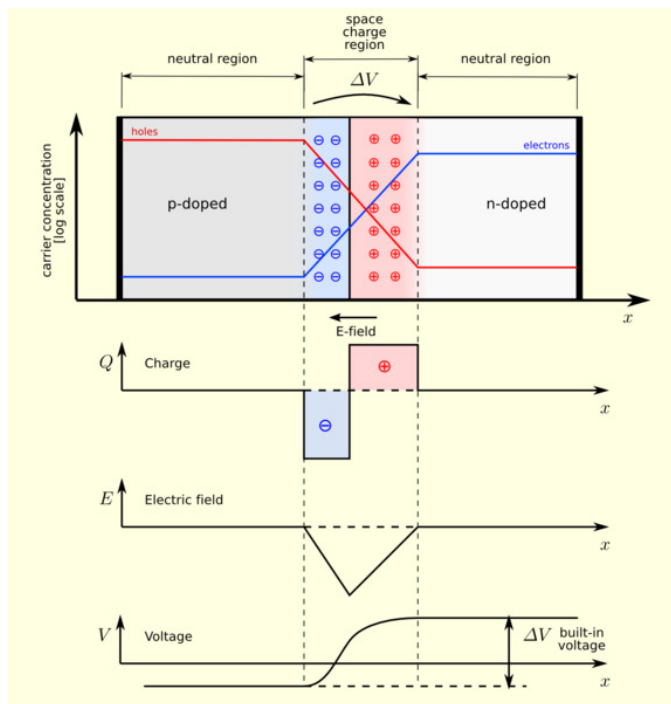
Charge is conserved during the depletion process, and the semiconductor remains electrically neutral as a whole. The depletion region has a bulk electric charge (space charge) density ρ related doping density by[7]

$$\rho_{\text{depletion region}} = \begin{cases} -eN_p = -eN_a & (p\text{-side}), \\ eN_n = eN_d & (n\text{-side}), \end{cases} \tag{1}$$

where $e > 0$ is the magnitude of the charge of an electron. Overall electrical neutrality implies that

$$\int_{p-\text{side}} \rho \, d\text{Vol} + \int_{n-\text{side}} \rho \, d\text{Vol} = 0. \tag{2}$$

Note that the depletion process can continue (with increased reverse-bias voltage) only so far as to fully deplete either the p-side or the n-side, depending on which side has the fewer total dopant atoms.

When a p-n junction is used as a detector of charged particles (or of photons) the junction is reverse biased such that ionization electrons (photoelectrons) drift toward the external contact on the n-side.[8] To maximum the volume over which ionization electrons can be

---

[7]The density of charge carriers drops to zero over distances of order 1 μm at the edges of the depletion region, as governed by thermal effects.

[8]In the language of particle detectors the n-side contact is called the anode, but in the language of semiconductor diodes (which must be forward biased to conduct) it is called the cathode.

quickly collected, it is desirable that the semiconductor be as fully depleted as possible.[9]

What is the minimum reverse-bias voltage for maximal depletion, and what is the electric field profile $E(x)$ for larger or smaller bias voltages?

2 Solution

We consider only 1-dimensional (x) dependence to the doping densities, and take coordinate x to run from the p-side to the n-side, with the n-side contact at potential $V > 0$ and the p-side contact at "ground".[10] In this convention the internal electric field is negative.

The one-dimensional electric field inside the device obeys Poisson's equation,

$$\boldsymbol{\nabla} \cdot \mathbf{E} = \frac{dE}{dx} = \frac{\rho(x)}{K\epsilon_0}, \tag{3}$$

where K is the (relative) dielectric constant ($K = 11.67$ for silicon).[11] The semiconductor extends from x_1 to x_2, with the p-n junction at x_0. The depletion region extends from x_p to x_n where $x_1 \leq x_p < x_0$ and $x_0 < x_n \leq x_2$. Integrating eq. (3) once, noting that the electric field is zero outside the depletion region, we obtain

$$E(x) = \begin{cases} 0 & (x_1 < x < x_p), \\ \int_{x_p}^{x} \frac{\rho(x')}{K\epsilon_0} \, dx' & (x_p < x < x_n), \\ 0 & (x_n < x < x_2). \end{cases} \tag{4}$$

Integrating eq. (4) over the whole device, and integrating by parts, we find

$$\begin{aligned} V & = V(x_2) - V(x_0) = V(x_2) = -\int_{x_1}^{x_2} E(x) \, dx = -\int_{x_p}^{x_n} dx \int_{x_p}^{x} \frac{\rho(x')}{K\epsilon_0} \, dx' \\ & = -x_n \int_{x_p}^{x_n} \frac{\rho(x)}{K\epsilon_0} \, dx + \int_{x_p}^{x_n} \frac{x\rho(x)}{K\epsilon_0} \, dx = \int_{x_p}^{x_n} \frac{x\rho(x)}{K\epsilon_0} \, dx, \end{aligned} \tag{5}$$

noting that charge conservation implies that

$$\int_{x_p}^{x_n} \rho(x) \, dx = 0. \tag{6}$$

For a specified reverse-bias voltage V, eqs. (5)-(6) determine the edges x_p and x_n of the depletion region, after which the internal electric-field distribution can be computed using eq. (4).

---

[9]The highest electric fields, which occur close to the p-n junction may be sufficient that the drifting ionization electrons initiate Townsend avalanches. In this case it would be desirable to deplete the p-side of the junction as fully as possible.

[10]Particle detectors are typically operated with the n-side contact at "ground" and the p-side contact at negative voltage.

[11]The relative dielectric constant is affected by the doping density N, but this effect is significant only for $N > 10^{17}/\text{cm}^3$ [12].

The highest voltage for which this model can apply is such that either $x_p = x_0$ or $x_n = x_2$. In practice, breakdown of the semiconductor under the high internal electric field occurs as voltages lower than this maximum, and we thereby avoid having to "fix" to model to apply at higher voltages. For p-n junctions used as particle detectors, with relatively thick depletion layers, the breakdown mechanism is Townsend avalanches (which avalanches are desirable if they don't lead to breakdown).

2.1 Constant Doping Densities

In the idealized case of constant doping densities, $N_p = N_d$ and $N_n = N_d$, eqs. (4)-(6) can be evaluated analytically.

Take the p-n junction to be at $x_0 = 0$. Then, eq. (6) tells us that

$$- x_p N_p = x_n N_n, \tag{7}$$

and eq. (5) becomes

$$V = \frac{e}{2K\epsilon_0}(x_p^2 N_p + x_n^2 N_n). \tag{8}$$

Hence, the depletion edges are given by

$$x_p = -\sqrt{\frac{2K\epsilon_0 V}{e} \frac{N_n}{N_p(N_p + N_n)}}, \qquad x_n = \sqrt{\frac{2K\epsilon_0 V}{e} \frac{N_p}{N_n(N_p + N_n)}}, \tag{9}$$

the width w of the depletion region is

$$w = x_n - x_p = \sqrt{\frac{2K\epsilon_0 V}{e} \frac{N_p N_n}{N_p + N_n}}. \tag{10}$$

The electric-field profile is triangular, with nonzero, negative values between x_p and x_n. The peak (negative) electric field is at the p-n junction, where

$$|E_{\max}| = \frac{N_n x_n}{K\epsilon_0} = \sqrt{\frac{2V}{eK\epsilon_0} \frac{N_p N_n}{N_p + N_n}}. \tag{11}$$

2.1.1 Junction Capacitance

As the reverse-bias voltage is raised from 0 to V, electric charge,

$$Q = eN_n x_n A = -eN_p x_p A, \tag{12}$$

flows through the external circuit as the charge carriers are swept out of the enlarging depletion region (leaving total charge $\pm Q$ in the n- and p-sides of the depletion region). The bias voltage (8) can also be written as

$$V = \frac{Q(x_n - x_p)}{K\epsilon_0 A} = \frac{Qw}{K\epsilon_0 A} \equiv \frac{Q}{C_{\text{junction}}}, \tag{13}$$

4

where the junction capacitance,

$$C = \frac{K\epsilon_0 A}{w},\tag{14}$$

is the same as that of a parallel-plate capacitor of width equal to the depletion width w (even though the charge $\pm Q$ does not reside on the edge surfaces of the depletion region but within its volume).

If the bias voltage is applied through a series resistor R_B, the time constant for changes in the bias voltage is $R_B C_{\text{junction}}$.

When the device detects an optical photon via creation of a photoelectron at the top surface of the p-layer, that photoelectron drifts towards the junction and generates an avalanche of electron-hole pairs, most of whose charge is produced close to the junction, over a distance $d \ll w$. As the electrons and holes of the avalanche separated under the influence of the internal electric field, their drift velocity depends on the local field strength as shown in the figures below (from [13]). These drift velocities are much higher than those of conduction electrons in metals; the electron drift velocity in Si "saturates" at $v_e \approx 10^7$ cm/s $= 0.1\ \mu$m/ps for fields larger than 10^4 V/cm.[12] The electron-hole charge separation has time scale d/v_e, which is a few tens of ps for an avalanche from a single photoelectron.
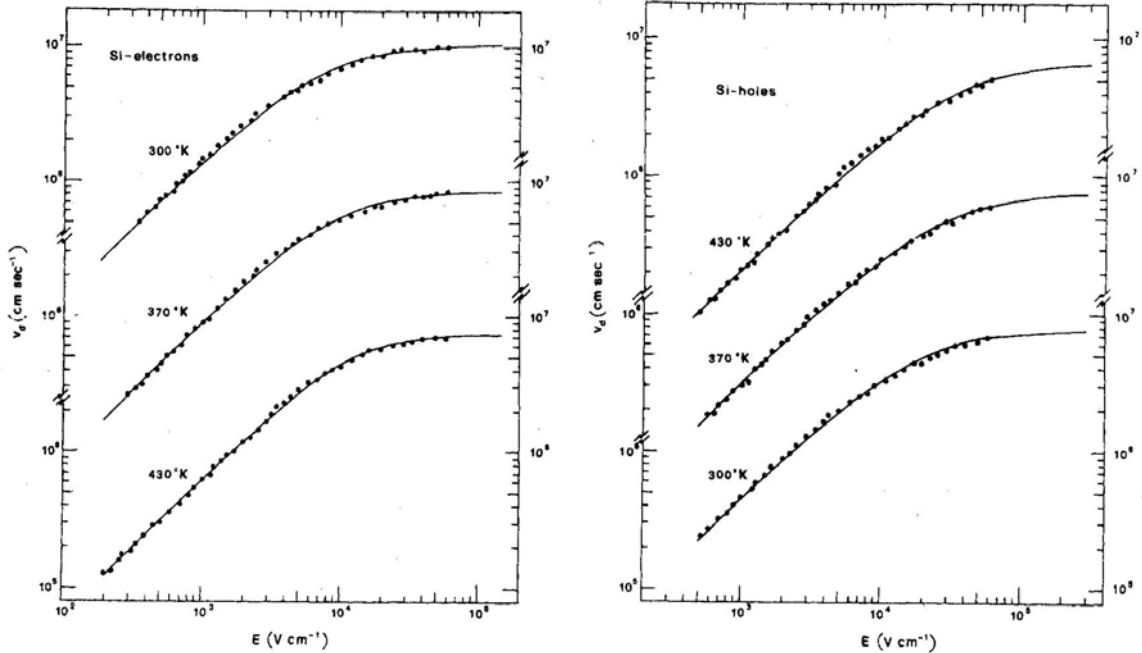
As the electrons and holes of the avalanche separate, the resulting electric field propagates away from the junction at speed c/K, and induces charge on the top and bottom surfaces

---

[12]Fits to the electron and hole drift velocities at room temperature have been given in [14], $v = \mu_0 E/[1 + N/(N/S + N_{\text{ref}}) + (E/A)^2/(e/A + F) + (E/B)^2]^{1/2}$, where E is the electric field strength in V/cm, N is the doping density per cm^3, and for electrons, $\mu_0 = 1400$ cm^2/V-s, $N_{\text{ref}} = 3 \times 10^{16}$/cm^3, $S = 350$, $A = 3500$ V/cm, $F = 8.8$, and $B = 7400$ V/cm, while for holes, $\mu_0 = 480$ cm^2/V-s, $N_{\text{ref}} = 4 \times 10^{16}$/cm^3, $S = 81$, $A = 6100$ V/cm, $F = 1.6$, and $B = 2500$ V/cm. For comparison of the fits with data, see
http://physics.princeton.edu/~mcdonald/LHC/Lu/ElectronVelocity_k.xlsx
http://physics.princeton.edu/~mcdonald/LHC/Lu/HoleVelocity_k.xlsx

of the APD. The avalanche acts as a kind of current source for this induced charge, which charges the APD capacitance on the time scale d/v_e, *i.e.*, over a few tens of ps. The voltage on the APD capacitance reaches $V_{\text{max}} = Ge/C_{\text{APD}}$, where G is the gain of the avalanche, over a rise time of d/v_e.

If this voltage is observed via a load resistor R_L, the time constant $R_L C_{\text{APD}}$ does not affect the rise time of the observed voltage provided $R_L C_{\text{APD}} \gg d/v_e$, but rather this time constant governs the exponential discharge of the APD capacitance, *i.e.*, it affects the fall time of the voltage signal.

Additional details of the APD readout circuitry are discussed in the Appendices.

2.2 Spatially Varying Doping Densities

2.2.1 Junction Capacitance

When doping densities N_p and N_n are functions of spatial coordinate x there is in general no closed-form expression for the dependence of the depletion width, $w = x_n - x_p$, on bias voltage V. However, from eq. (5) we see that a change δV in the bias voltage results in a flow of charge $\delta Q \approx \rho(x_n) A \, dx_n = -\rho(x_p) A \, dx_p$ off of the device as related by

$$\delta V \approx \frac{x_n \rho(x_n) \, dx_n}{K\epsilon_0} - \frac{x_p \rho(x_p) \, dx_p}{K\epsilon_0} = \frac{\delta Q (x_n - x_p)}{K\epsilon_0 A} = \frac{\delta Q w}{K\epsilon_0 A} = \frac{\delta Q}{C_{\text{junction}}}. \tag{15}$$

Hence, the junction capacitance, $C_{\text{junction}} = K\epsilon_0 A/w$, again governs the time constant for changes in the bias voltage.

2.2.2 Example: an Avalanche Photodiode

As an example of a *p-n* junction in which the doping densities vary with position we consider the 8×8 mm^2 avalanche photodiode described in [15]. The junction is 300 μm thick, with $w = 60$ μm of deep-diffused *p*-doping on a substrate with uniform *n*-doping. The doping densities are illustrated on the left figure below.
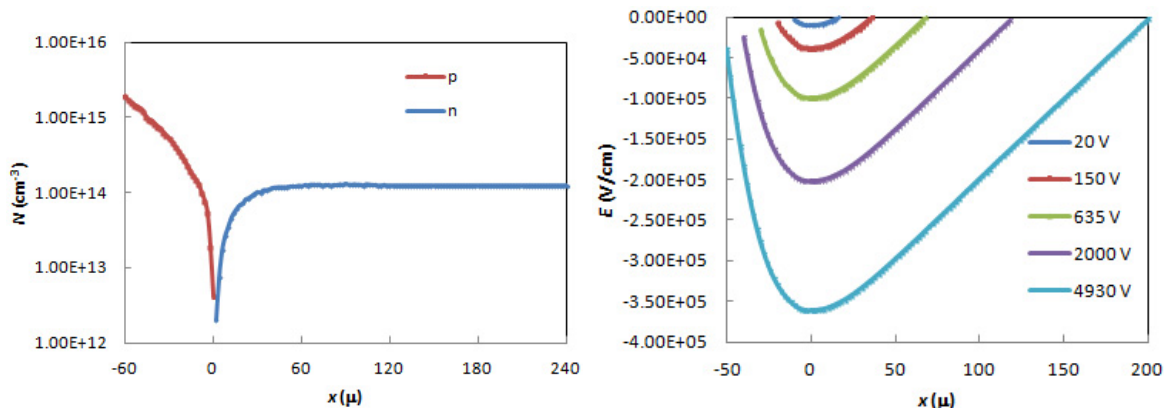
The interior electric field is estimated via the simplified model of eq. (4) by beginning the integration at $x_p = -10, -20, -30, -40,$ and -50 μm, leading to the electric-field distributions shown in the right figure above. The reverse-bias voltage across the junction is obtained by integration of the electric field. Because of very large *p*-doping density near

6

$x = -60$ μm, moving the p-side depletion edge to slightly less than -50 μm results in the n-side becoming completely depleted, at around 5000 V bias voltage. In practice, internal breakdown limits the voltage in this device to about 1900 V (and the peak electric field magnitude to $\approx 2 \times 10^5$ V/cm).

For bias voltage of 1700 V, the width of the depletion region (where $E < 0$ in the above right figure) is $w \approx 150$ μn, and the nominal device capacitance is

$$C_{\text{APD}} = C_{\text{junction}} = \frac{K\epsilon_0 A}{w} = \frac{11.67 \cdot 8.85 \times 10^{-12} \cdot 64 \times 10^{-6}}{150 \times 10^{-6}} = 44 \text{ pf.} \qquad (16)$$

Studies (G. Atoian, private communication) of the 8×8 mm^2 APD, using a Ru^{106} β-source showed a 90-10 fall time of 7.2 ns $= 2.2 R_L C_{\text{APD}}$.[13] For the preamp used, $R_L = 50$ Ω, so we infer that $C_{\text{APD}} = 55$ pf, compared to 44 pf according to eq. (16).[14]

In the Appendices below we will use $C_{\text{APD}} = 60$ pf for the 8×8 mm^2 APD.

---

[13]Because the observed pulse was negative, the trailing edge was rising, and what we call the fall time was reported as the rise time by the oscilloscope analysis package.

[14]This discrepancy cannot be attributed to the frequency dependence of the relative dielectric constant K of silicon, which remains near 10 up to 1 GHz frequency.
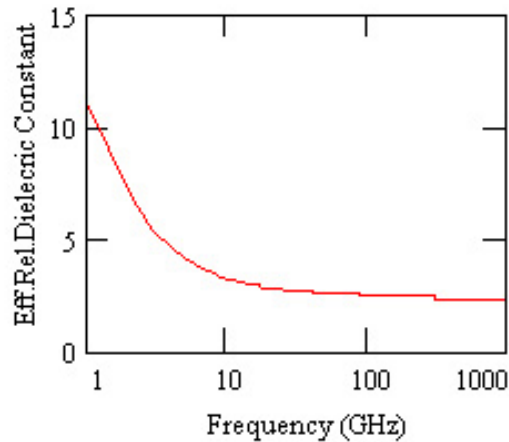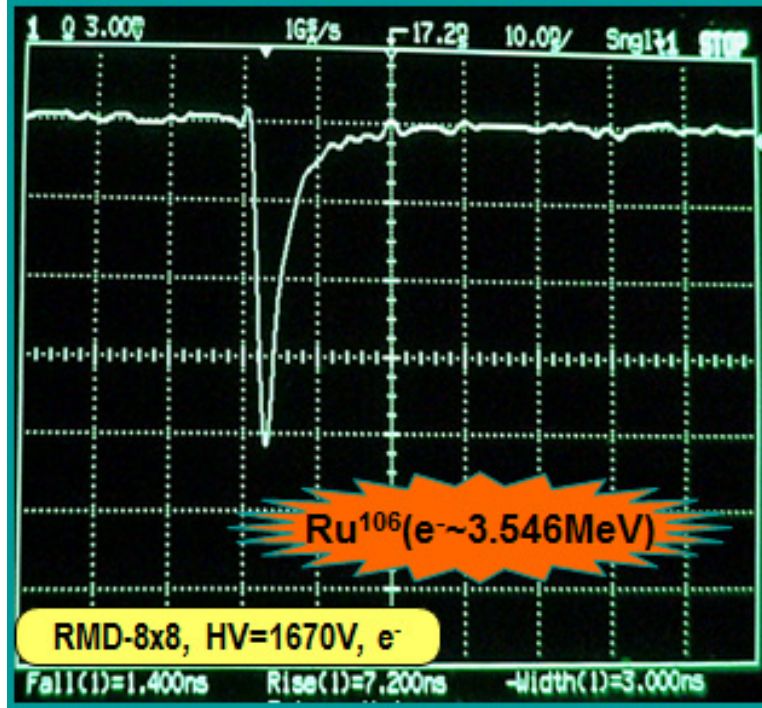
A   Gain in an Avalanche Photodiode

A.1   McIntyre's Gain Model

Relatively large currents were observed in reverse-biased Si and Ge *p-n* junctions when bombarded by α-particles by McKay and McAfee in 1953 [17], which was interpreted as the result of Townsend avalanches in the high-field region near the junction, initiated by electrons (and holes!) generated by impact ionization. An analysis of the gain (multiplication factor) in this process was given by Miller in 1955 [20], based on the Townsend (impact ionization) coefficients $\alpha(E)$ and $\beta(E)$ for electrons and holes, respectively. That is, $n_e(x)$ electrons at position x (perpendicular to the junction, parallel to the electric field E) become "multiplied" according to

$$n_e(x + dx) = n_e(x)\,\alpha(E(x))\,dx, \tag{17}$$

after traversing distance dx opposite to the direction of the field $\mathbf{E}$.[15] Of course, each impact ionization creates an electron-hole pair, so the holes are "multiplied" also. Similarly, $n_h(x)$ holes at position x become "multiplied" (to

$$n_h(x - dx) = n_h(x)\,\alpha(E(x))\,(-dx), \tag{18}$$

after traversing distance dx in the direction of the field $\mathbf{E}$ (with an equal number of holes created as well).

---

[15]Conventions differ as to whether the electric field $\mathbf{E}$ is in the positive or negative x-direction. Here, we suppose that electrons moves in the positive x-direction, and that $\mathbf{E}$ points in the negative x-direction.

If the junction extends from $x_p < 0$ to $x_n > 0$, and an electron-hole pair is somehow created at position x inside the junction, as the electron drifts to $x = x_n$ and the holes drifts to $x = x_p$, the number of secondary electron-hole pairs created by impact ionization is

$$N(x) = \int_x^{x_n} \alpha(x')\,dx' + \int_x^{x_p} \beta(x')\,(-dx') = \int_x^{x_n} \alpha(x')\,dx' + \int_{x_p}^x \beta(x')\,dx'. \tag{19}$$

However, if a (secondary) electron-hole pair is generated at position x', as the new electron and hole drift to the ends of the junction, additional (tertiary) electron-hole pairs are created.

We seek the total number $M(x)$ of electron-hole pairs in the junction associated with an initial pair at position x. Then, $M(x')\,\alpha(x')\,dx'$ is the total number of electron-hole pairs created somewhere in the junction due to the creation of $\alpha(x')\,dx'$ secondary pairs in the interval dx' with $x' > x$, and similarly $M(x')\,\beta(x')\,dx'$ is the total number of electron-hole pairs created somewhere in the junction due to the creation of $\beta(x')\,dx'$ secondary pair in the interval dx' with $x' < x$. Altogether, the total number of electron-hole pairs somewhere in the junction associated with the initial pair at x is given by

$$M(x) = 1 + \int_x^{x_n} M(x')\,\alpha(x')\,dx' + \int_{x_p}^x Mx\,\beta(x')\,dx', \tag{20}$$

as first deduced by McIntyre (1966) [18].[16]

The integral equation (20) was cleverly solved in [18] by first taking the derivative,[17]

$$\frac{dM(x)}{dx} = -M(x)\,[\alpha(x) - \beta(x)], \tag{21}$$

which has the formal solution

$$M(x) = M(x_p)\,e^{-\int_{x_p}^x (\alpha-\beta)\,dx'} = M(x_n)\,e^{\int_x^{x_n} (\alpha-\beta)\,dx'}. \tag{22}$$

Using eq. (22) in eq. (20) for $x = x_p$ (and also for $x = x_n$), we find

$$M(x_p) = \frac{1}{1 - \int_{x_p}^{x_n} dx'\,\alpha\,e^{-\int_{x_p}^{x'} (\alpha-\beta)\,dx''}}, \qquad M(x_n) = \frac{1}{1 - \int_{x_p}^{x_n} dx'\,\beta\,e^{\int_{x'}^{x_n} (\alpha-\beta)\,dx''}}, \tag{23}$$

and using these forms in eq. (22) we obtain the gain (multiplication factor) $M(x)$ for an electron-hole pair somehow created at x,

$$M(x) = \frac{e^{-\int_{x_p}^x (\alpha-\beta)\,dx'}}{1 - \int_{x_p}^{x_n} dx'\,\alpha\,e^{-\int_{x_p}^{x'} (\alpha-\beta)\,dx''}} = \frac{e^{\int_x^{x_n} (\alpha-\beta)\,dx'}}{1 - \int_{x_p}^{x_n} dx'\,\beta\,e^{\int_{x'}^{x_n} (\alpha-\beta)\,dx''}}. \tag{24}$$

If either α or β is zero there is no tertiary production of electron-hole pairs, and eq. (24) simplifies to $M(x)_{\beta=0} = e^{\int_x^{x_n} \alpha\,dx'}$ and $M(x)_{\alpha=0} = e^{\int_{x_p}^x \beta\,dx'}$, as expected.

---

[16]Earlier discussions considered only $M(x_n)$ of eq. (23): McKay [19] assumed that $\alpha = \beta$, while Miller [20] supposed they we not equal.

[17]When considering currents in the junction rather than individual electrons and holes, eq. (21) is often interpreted as describing the spatial variation of the currents. See, for example, [21], p. A768.

When both α and β are nonzero (as holds generally) and large (as occurs for high electric fields), it is possible that the tertiary production of electron hole pairs proceeds without limit. In practice, if the number of electron-hole pairs becomes very large, they modify the electric field inside the junction, which "breaks down".

The model gives an indication of this in that $M(x)$ diverges as either $\int_{x_p}^{x_n} dx' \, \alpha \, e^{-\int_{x_p}^{x'}(\alpha-\beta)\,dx''}$ or $\int_{x_p}^{x_n} dx' \, \beta \, e^{\int_{x'}^{x_n}(\alpha-\beta)\,dx''}$ approaches 1 (and becomes meaningless for larger values of these integrals).

For example, if $\alpha = \beta$, and the electric field is uniform across the junction of width $w = x_n - x_p$, then $M \to \infty$ when $\alpha w = 1$. That is, if a single secondary electron-hole pair is generated in the junction, this leads to a single tertiary pair, which leads to a single quaternary pair, etc., and the gain diverges.

As will be reviewed in Appendix A.2, in silicon $\beta \ll \alpha$. If we suppose that $\beta = k\alpha$ with $k \ll 1$, and that the electric field is uniform, then the gain diverges when $\alpha w \approx -\ln k = \ln(\alpha/\beta) = $ a few.

In practice, the junction becomes unstable well before the gain becomes infinite. We conjecture that a "rule of thumb" is that the junction becomes unstable when the gain $M(x_p)$ becomes slightly larger than α/β.

The model of McIntyre has been elaborated upon in various ways, by McIntyre himself [22, 23, 24], and by others (see, for example, [25]).

A.2 α and β

B Current Pulse in an Avalanche Photodiode

An equivalent circuit for an avalanche photodiode (APD), when connected to a load such as a preamp with input impedance R_{load}, is shown below.
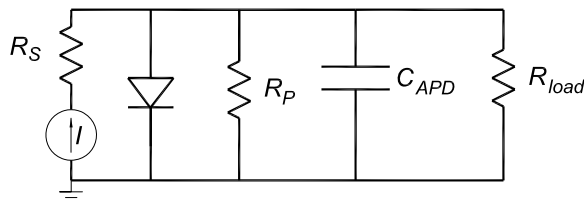
The avalanche in the junction region is represent as a current source $I(t)$ with a small series resistance R_S. The junction capacitance discussed in sec. 2.1.1 is indicated as C_{APD}. The junction is also shown as a diode (which is not active when reverse biased). There also exists a large parallel resistance R_P, which has little effect on the short pulses considered here.

B.1 Single Photoelectron

If a single optical photon is incident on the top surface of the avalanche photodiode and a photoelectron is generated, the latter drifts towards the junction and eventually creates an avalanche. The extent of the avalanche is roughly that of the junction, i.e., a few microns. The velocity of electrons (and holes) near the junction, where the electric field strength is about 10^4 V/cm for typical operation, is "saturated" with values closed to 10^7 cm/s $=$

0.1 μm/ps. Hence, the avalanche lasts a few tens of ps, which is the characteristic time scale of the current pulse (inside the avalanche photodiode) from a single photoelectron.

On this short time scale, the impedance of the capacitance C_{APD} is much less than R_{load}, so the immediate response of the circuit is that the capacitor charges up to voltage $V = Q/C_{\text{APD}}$, where $Q = Ge$ with G being the gain of the APD and e the charge of an electron. The voltage waveform for the load resistor has a rise time of a few tens of ps, and a fall time with time constant $R_{\text{load}}C_{\text{APD}}$ as the capacitor discharges.

B.2 Response to a Penetrating Charged Particle

If a high-energy charged particle passes through the APD, it creates a trail of electron-hole pairs. A so-called minimum-ionizing charged particle creates about $N_{\text{min}} = 100$ electron-holes pairs per micron.

For the APD considered in sec. 2.2.2, about 6000 electron-holes pairs are created by a minimum-ionizing particle that passes through the 60-μm-thick p-side. However, the electric field near the top of the APD is lower than 10^4 V/cm, such that the initial drift velocity of ionization electrons in this region is low, and they do not contribute to the "prompt" signal. For such an APD biased around 2000 V, we suppose that the effective thickness of the APD for its "prompt" signal is $d_{\text{eff}} \approx 40$ μm, so that some $N_{\text{min}}d_{\text{eff}} = 4000$ ionization electrons move at the saturated drift velocity towards the junction, arriving of an interval about 400 ps long.

The corresponding current pulse $I(t)$ is approximately flat for time interval $\Delta_1 \approx 400$ ps (with initial and final transients lasting a few tens of ps). That is, the current pulse is approximately

$$I_1(t) = \begin{cases} 0 & (t < 0), \\ I_0 & (0 < t < \Delta_1), \\ 0 & (t > \Delta_1), \end{cases} \tag{25}$$

taking the avalanche to start at time $t = 0$.
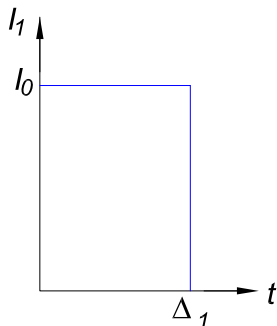
If the discharge time constant $R_{\text{load}}C_{\text{APD}}$ is large compared to 400 ps, the initial effect of the current pulse is again to charge the capacitor to voltage Q/C_{APD} where $Q = I_0\Delta_1 = GN_{\text{min}}d_{\text{eff}}$, after which the charge flows off the capacitor through the load resistor. However, for small R_{load}, some of the charge flows off the capacitor through the resistor before its voltage reaches Q/C_{APD}. In either case, the voltage rise time is 400 ps, although if the load

resistor represents an amplifier with a finite bandwidth the observed rise time will be slower, as will be illustrated in sec. B.3.

B.3   Response to a Pulse of Infrared Photons

Infrared photons with wavelength around 1 μm have an absorption length greater than the thickness of the p-side of the avalanche photodiode, so they can create photoelectrons at any depth in the p-layer with approximate the same probability. Of course, a single infrared photon can create only one photoelectron, for which the avalanche current pulse would be the same as that discussed in sec. A.1. However, a beam of infrared photons of sufficient intensity can create a track of photoelectron, closely approximating the effect of a charged particle. Here, we consider a beam if infrared photons that has width Δ_γ in time, for which the intensity $vs.$ time can be written

$$
N_\gamma(t) = \begin{cases} 0 & (t < 0), \\ N_0 & (0 < t < \Delta_\gamma), \\ 0 & (t > \Delta_\gamma). \end{cases} \tag{26}
$$

The avalanche current pulse from such a beam of photons is the convolution

$$
I_\gamma(t) = \int_{-\infty}^{t} dt' \, N_\gamma(t') I_1(t - t') = N_0 \int_0^{\min(t, \Delta_\gamma)} dt' \, I_1(t - t') = N_0 I_0 \int_{\max(0, t - \Delta_1)}^{\min(t, \Delta_\gamma)} dt'. \tag{27}
$$

The result is slightly different for cases $\Delta_\gamma < \Delta_1$ and $\Delta_1 < \Delta_\gamma$, but can be written in a single form if we define $\Delta_{\text{lo}} = \min(\Delta_\gamma, \Delta_1)$ and $\Delta_{\text{hi}} = \max(\Delta_\gamma, \Delta_1)$

$$
I_\gamma(t) = N_0 I_0 \begin{cases} 0 & (t < 0), \\ t & (0 < t < \Delta_{\text{lo}}), \\ \Delta_{\text{lo}} & (\Delta_{\text{lo}} < t < \Delta_{\text{hi}}), \\ \Delta_{\text{lo}} + \Delta_{\text{hi}} - t & (\Delta_{\text{hi}} < t < \Delta_{\text{lo}} + \Delta_{\text{hi}}), \\ 0 & (t > \Delta_{\text{lo}} + \Delta_{\text{hi}} = \Delta_\gamma + \Delta_1). \end{cases} \tag{28}
$$
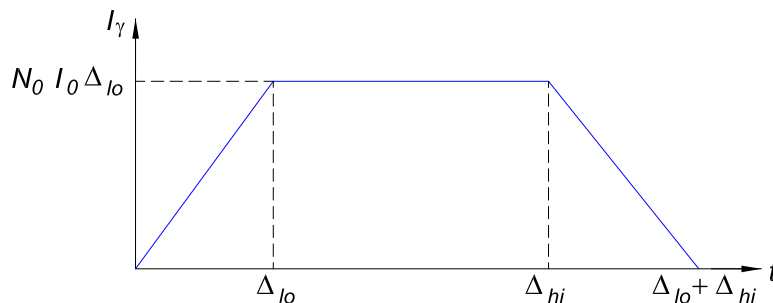
C   Load Voltage via Laplace Transforms

We can use the method of Laplace transforms to solve for the load voltage, $V_L = I_L R_L$, for various hypothesis as to the current pulse $I(t)$ from an avalanche at the junction. We will ignore the large parallel resistance R_P (and the junction diode, which plays no role for a reverse-biased APD). Then, the voltage and current circuit associated with the equivalent circuit shown on p. 6 are

$$V_R = I_L R_L = \frac{Q_C}{C}, \qquad I_C = \dot{I}_L R_L C, \qquad I = I_C + I_L = I_L + \dot{I}_L R_L C. \tag{29}$$

Writing that Laplace transform of a function $F(t)$ as

$$\mathcal{L}(F) = f(s) = \int_0^\infty e^{-st} F(t) \, dt, \tag{30}$$

and noting that the Laplace transform of the time derivative $\dot{F}$ is

$$\mathcal{L}(\dot{F}) = \int_0^\infty e^{-st} \dot{F}(t) \, dt = -F(0) + s \int_0^\infty e^{-st} F(t) \, dt = sf - F(0), \tag{31}$$

the Laplace transform of the last of eq. (29) is

$$i = i_L + i_L s R_L C, \qquad v_L = i_L R_L = \frac{i R_L}{1 + s R_L C}, \tag{32}$$

where we suppose that $t = 0$ is the time at which the current pulse begins, such that $I(0) = 0$. Then, the load voltage is the inverse Laplace transform of eq. (32),

$$V_L = \mathcal{L}^{-1}(v_L) = \mathcal{L}^{-1}\left(\frac{i R_L}{1 + s R_L C}\right). \tag{33}$$

As an example, suppose the current pulse is a delta function $I(t) = Q_0 \, \delta(t)$, where $Q_0 = \int I \, dt$ is the total charge in the pulse. Then, $i = \int e^{-st} Q_0 \delta(t) \, dt = Q_0$, and

$$V_L = Q_0 R_L \mathcal{L}^{-1}\left(\frac{1}{1 + s R_L C}\right) = \frac{Q_0}{C} e^{-t/R_L C} = V_0 \, e^{-t/R_L C}, \tag{34}$$

where $V_0 = Q_0/C$ is the voltage across the capacitor at the end of the current pulse, at which time charge Q_0 is on the capacitor.[18] This is, of course, the usual result for the voltage across a resistor in parallel with a capacitor.

C.1   Effect of Adding a Series Capacitance

The fall time, but not the peak voltage, can be lowered by adding a capacitor in series with the load resistor.

---

[18]Note that for $F(t) = e^{-t/\tau}$, its Laplace transform is $f = \int_0^\infty e^{-st} e^{t/\tau} \, dt = \tau/(1 + s\tau)$.
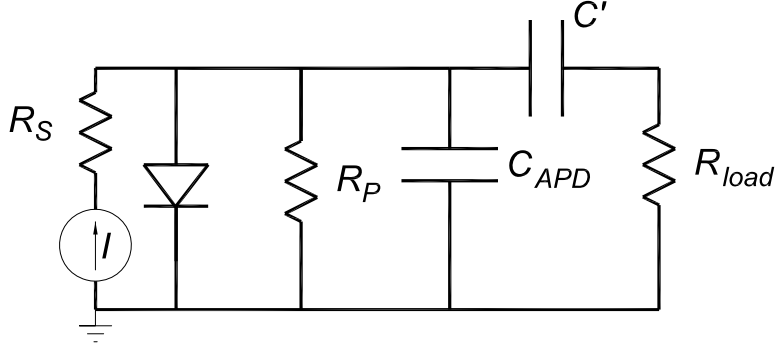
In this case the circuit equations (29) become (again neglecting the large parallel resistance R_P),

$$V_R = I_L R_L + \frac{Q'}{C'} = \frac{Q_C}{C}, \quad I_C = \dot{I}_L R_L C + I_L \frac{C}{C'}, \quad I = I_C + I_L = I_L \frac{C + C'}{C'} + \dot{I}_L R_L C. \quad (35)$$

The Laplace transformed equations are,

$$i = i_L \frac{C}{C_{\text{eff}}} + i_L s R_L C, \qquad C_{\text{eff}} = \frac{CC'}{C + C'}, \qquad v_L = i_L R_L = \frac{C_{\text{eff}}}{C} \frac{i R_L}{1 + s R_L C_{\text{eff}}}, \qquad (36)$$

which have the same form of dependence on s as eq. (33).

For the example of a delta-function current pulse, where $i = Q_0$, the load voltage can be transcribed from eq. (34) as

$$V_L(t > 0) = \frac{C_{\text{eff}}}{C} \frac{Q_0}{C_{\text{eff}}} e^{-t/RC_{\text{eff}}} = \frac{Q_0}{C} e^{-t/RC_{\text{eff}}}. \qquad (37)$$

C.2 Effect of Load Bandwidth of a Voltage Amplifier

The load resistor may represent the input impedance of a voltage amplifier that has a limited bandwidth.

We can approximate the bandwidth limitation as due to low-pass, RC filter, as shown below, where all the input current flows onto the filter capacitor C_b after passing through the filter resistor R_b.
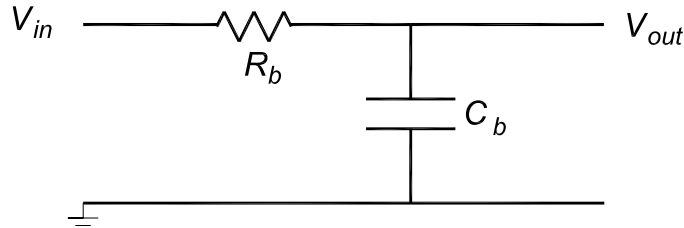
The circuit equations are

$$V_{\text{in}} = I_{\text{in}} R_b + \frac{Q_C}{C_b}, \qquad \dot{V}_{\text{in}} = \dot{I}_{\text{in}} R_b + \frac{I_{\text{in}}}{C_b}, \qquad V_{\text{out}} = \frac{Q_C}{C_b}, \qquad \dot{V}_{\text{out}} = \frac{I_{\text{in}}}{C_b}. \qquad (38)$$

The Laplace transformed equations are

$$s v_{\text{in}} = s i_{\text{in}} R_b + \frac{i_{\text{in}}}{C_b}, \quad i_{\text{in}} = \frac{s v_{\text{in}} C_b}{1 + s R_b C_b}, \quad s v_{\text{out}} = \frac{i_{\text{in}}}{C_b}, \quad v_{\text{out}} = \frac{v_{\text{in}}}{1 + s R_b C_b} \equiv \frac{v_{\text{in}}}{1 + s \tau_b}. \qquad (39)$$

14

The factor $T(s) = 1/(1 + s\tau_b)$, where $\tau_b \equiv R_b C_b$, is called the transfer function of the filter, whose bandwidth is defined as $1/2\pi\tau_b$.[19,20]

If the load resistor R_L represents the input impedance of an amplifier of voltage gain G and bandwidth $\nu = 1/2\pi\tau_b$ (in ordinary frequency), the output voltage from an APD with added series capacitance C' has Laplace transform

$$v_{\rm out} = G\frac{v_{\rm in}}{1 + s\tau_b} = G\frac{C_{\rm eff}}{C}\frac{iR_L}{1 + sR_LC_{\rm eff}}\frac{1}{1 + s\tau_b} \qquad \text{with} \qquad C_{\rm eff} = \frac{CC'}{C + C'}. \tag{42}$$

For example, in case of a delta-function current pulse with Laplace transform $i = Q_0$, the output voltage follows from the inverse Laplace transform of eq. (42) as

$$V_{\rm out} = GQ_0\frac{R_LC_{\rm eff}}{C}\frac{e^{-t/R_LC_{\rm eff}} - e^{-t/\tau_b}}{R_LC_{\rm eff} - \tau_b} \qquad \text{with} \qquad C_{\rm eff} = \frac{CC'}{C + C'}, \tag{43}$$

assuming that $R_LC_{\rm eff} > \tau_b$, i.e., that the amplifier bandwidth is large.

The figure below illustrates the output voltage for $C = 60$ pf, $C' = 38$ pf, $C_{\rm eff} = 23$ pf, $R_L = 50\ \Omega$, and amplifier bandwidths of ∞, 1 GHz ($\tau_b = 160$ ps) and 500 MHz ($\tau_b = 320$ ps).[21]

---

[19]Filters with more components can have a sharper frequency cutoff. For example, a 3rd-order Butterworth filter has the transfer function $1/(1 + s\tau)(1 + s\tau + s^2\tau^2)$.

[20]A useful result is that a Laplace transform $f(s)$ of a function $F(t)$ that is zero to $t < 0$ is also its Fourier integral transform f_ω, if we take $s = j\omega$, where $j = \sqrt{-1}$ in the electrical-engineering convention,

$$f(j\omega) = \int_0^\infty e^{-j\omega t}F(t)\,dt = \int_{-\infty}^\infty e^{-j\omega t}F(t)\,dt = f_\omega. \tag{40}$$

The gain $G(\omega)$ of the filter (a number less than 1) as a function of angular frequency ω is taken to be the magnitude of the output voltage for unit input voltage at that frequency. That is,

$$G(\omega) = |T(j\omega)| = \sqrt{T(j\omega)T^\star(j\omega)} = \sqrt{T(j\omega)T(-j\omega)} = \sqrt{\frac{1}{1 + \omega^2\tau_b^2}} \tag{41}$$

The cutoff (angular) frequency of the filter is taken to be $\omega_c = 1/\tau_b$, such that $\tau_b = 1/2\pi\nu_c$ where $\nu_c = 2\pi\omega_c$ is the ordinary cutoff frequency. For example, with $\nu_c = 500$ MHz, $\tau_F = 1/\pi$ ns $= 318$ ps.

As the cutoff frequency the output voltage is reduced by $1/sqrt2$, so the output power is $1/2$ of the input power. As such, ν_c is called the 3-dB cutoff frequency, and also called the bandwidth of the filter.

[21]In this figure, and that on p. 13, the total charge in the pulse is $Q = N_{\rm min}d_{\rm eff} = 100 \cdot 40 = 4000$ electrons, multiplied by APD gain of $G_{\rm APD} = 200$ and by readout amplifier gain of $G_{\rm amp} = 316$ (power gain of 50 dB).

Delta–function pulse, $R_L = 50\ \Omega$, $C = 60$ pf, $C' = 38$ pf, $C_{\text{eff}} = 23$ pf
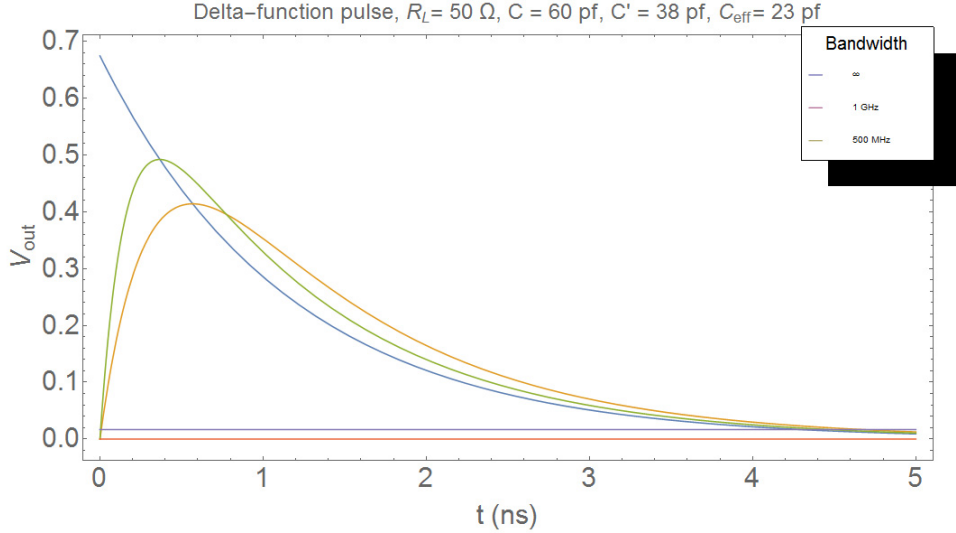
The 10-90 rise times are roughly $2\tau_b$. The peak voltage in this example drops from 0.68 V for infinite bandwidth to 0.42 V for 500-MHz bandwidth.

C.3 Penetrating Charged Particle

As in sec. A.2, we consider that case of a single charged particle that passes through the APD, which generates a current pulse $I_1(t)$ at the junction given by eq. (25). The Laplace transform of this current pulse is

$$\mathcal{L}(I_1) = i_1 = \int_0^{\Delta_1} e^{-st} I_0\, dt = \frac{I_0}{s}(1 - e^{-s\Delta_1}) = \frac{Q_0}{s\Delta_1}(1 - e^{-s\Delta_1}), \tag{44}$$

where $Q_0 = I_0\Delta_1$ is the total charge in the current pulse. The load voltage (33) can be evaluated analytically using the Wolfram Alpha Inverse Laplace Transform Calculator,

$$V_L(t > 0) = \frac{Q_0 R_L}{\Delta_1}\mathcal{L}^{-1}\left(\frac{1 - e^{-s\Delta_1}}{s(1 + sR_L C)}\right) = \frac{Q_0 R_L}{\Delta_1}\left(1 - e^{-t/R_L C} + \theta(t - \Delta_1)(e^{(\Delta_1 - t)/R_L C} - 1)\right), \tag{45}$$

where $\theta(t) = 0$ for $t < 0$ and 1 for $t > 0$. That is,

$$V_L(t > 0) = \frac{Q_0 R_L}{\Delta_1}\begin{cases} 1 - e^{-t/R_L C} & (t < \Delta_1), \\ e^{-t/R_L C}(e^{\Delta_1/R_L C} - 1) & (t > \Delta_1). \end{cases} \tag{46}$$

The load voltage rises to a maximum at time $t = \Delta_1$, after which it decays exponentially with time constant $R_L C$.

The full rise time of the waveform is just Δ_1 (independent of $R_L C$), so the 90-10 rise time is about $0.8\Delta_1$ when $\Delta_1 \ll R_L C$ (so about 320 ps for the APD considered in sec. 2.2.2),[22] while the 90-10 fall time is $2.2 R_L C$ (as usual for exponential decay).

---

[22]When $\Delta_1 > R_L C$ the full rise time is still Δ_1, but the rising waveform $1 - e^{-t/R_L C}$ would perhaps be better characterized as having time constant $R_L C$.

16

The peak voltage across the load is

$$V_{\max} = \frac{Q_0 R_L}{\Delta_1}(1 - e^{-\Delta_1/R_L C}) \approx \frac{Q_0}{C}, \tag{47}$$

where the approximation holds when $\Delta_1 \ll R_L C$. Thus, the peak voltage is unaffected by the load resistance, but varies inversely with the (effective) capacitance of the APD.

If the load resistor R_L represents the input impedance of an amplifier of voltage gain G and bandwidth $\nu = 1/2\pi\tau_b$ (in ordinary frequency), the output voltage from an APD with added series capacitance C', the output voltage is

$$\begin{aligned}
V_{\text{out}} &= G\frac{C_{\text{eff}}}{C}\frac{Q_0 R_L}{\Delta_1}\mathcal{L}^{-1}\left(\frac{1 - e^{-s\Delta_1}}{s(1 + sR_L C_{\text{eff}})(1 + s\tau_b)}\right) \\
&= G\frac{C_{\text{eff}}}{C}\frac{Q_0 R_L}{\Delta_1}\left[1 + \frac{\tau e^{-t/\tau_b} - R_L C_{\text{eff}} e^{-t/R_L C_{\text{eff}}}}{R_L C_{\text{eff}} - \tau_b}\right. \\
&\left. +\theta(t - \Delta_1)\left(\frac{R_L C_{\text{eff}} e^{(\Delta_1-t)/R_L C_{\text{eff}}} - \tau_b e^{(\Delta_1-t)/\tau_b}}{R_L C_{\text{eff}} - \tau_b} - 1\right)\right]. \tag{48}
\end{aligned}$$

That is,

$$V_L(t > 0) = G\frac{C_{\text{eff}}}{C\Delta_1}\frac{Q_0 R_L}{R_L C_{\text{eff}} - \tau_b}
\begin{cases}
R_L C_{\text{eff}}(1 - e^{-t/R_L C_{\text{eff}}}) - \tau_b(1 - e^{-t/\tau_b}) & (t < \Delta_1), \\
R_L C_{\text{eff}} e^{-t/R_L C_{\text{eff}}}(e^{\Delta_1/R_L C_{\text{eff}}} - 1) & \\
\quad -\tau_b e^{-t/\tau_F}(e^{\Delta_1/\tau_b} - 1) & (t > \Delta_1),
\end{cases} \tag{49}$$

The figure below illustrates the output voltage for $C = 60$ pf, $C' = 38$ pf, $C_{\text{eff}} = 23$ pf, $R_L = 50\ \Omega$, $\Delta_1 = 400$ ps, and amplifier bandwidths of ∞, 1 GHz ($\tau_b = 160$ ps) and 500 MHz ($\tau_b = 320$ ps).

Rectangular pulse, $\Delta_1 = 0.4$ ns, $R_L = 50\ \Omega$, $C = 60$ pf, $C' = 38$ pf, $C_{\text{eff}} = 23$ pf
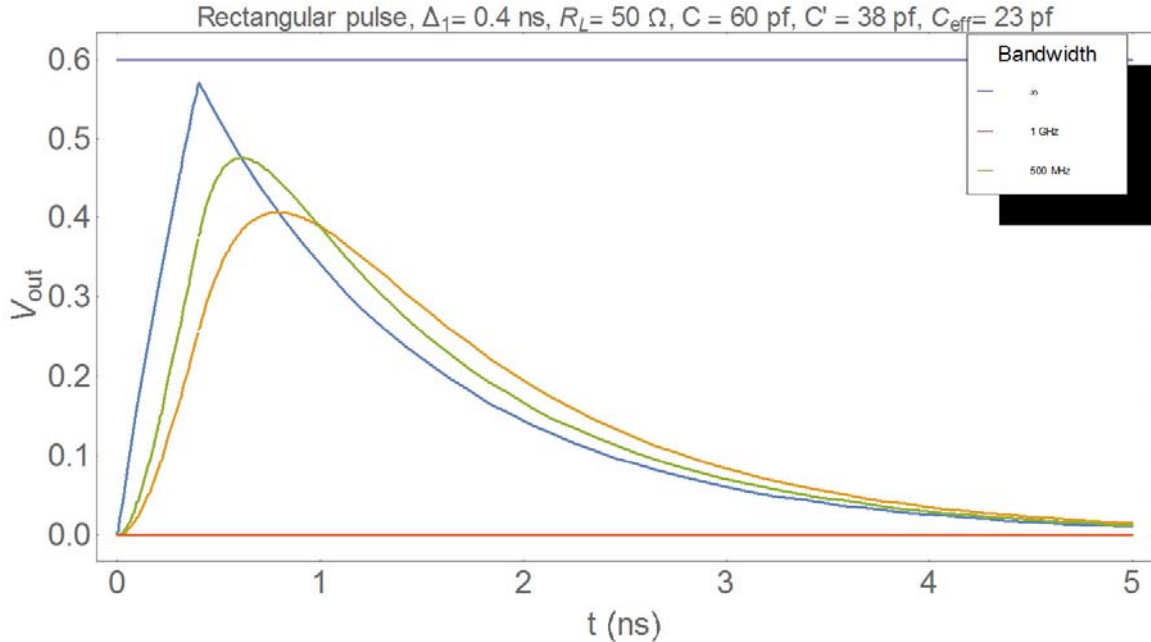
The 10-90 rise times are only slightly larger than the width Δ_1 of the (rectangular) avalanche current pulse, and the peak voltages are only slightly less than for a delta-function pulse of the same total charge (p. 12).

However, if the load resistor is only 5 Ω, then the peak voltage is considerably reduced, as shown in the figure below. As such, there is an optimum value of the load resistor for best signal to noise, when the limiting noise is the Johnson (thermal) noise of the resistor.

Rectangular pulse, Δ_1= 0.4 ns, R_L = 5 Ω, C = 60 pf C' = 38 pf, C_{eff}= 23 pf
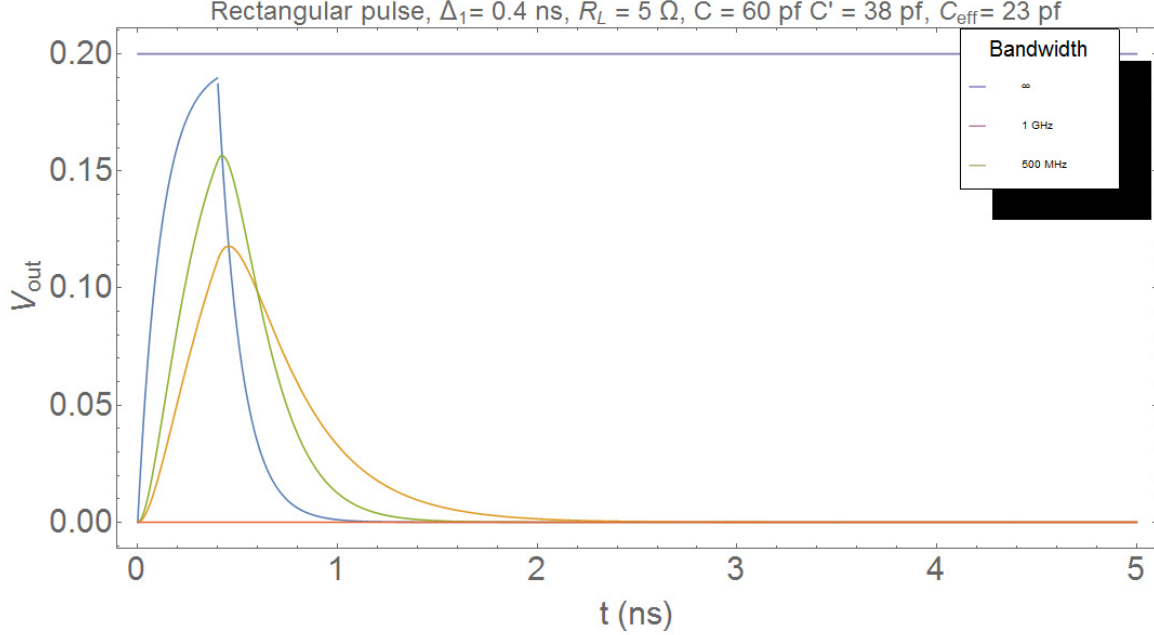
D   Time Resolution

A time can be assigned to the output waveform from the APD as the moment when the leading edge of that waveform reaches some specified voltage (or some specified fraction of the maximum voltage V_{max}. In the approximation that the leading edge of the waveform is a straight line of slope V_{max}/Δ, where $\Delta \approx d/v_e$ is the full rise time, the rms time resolution σ_t can be related to the rms noise voltage σ_V according to

$$\sigma_t = \frac{\Delta}{V_{\text{max}}}\sigma_V \approx \frac{d}{v_e}\frac{C_{\text{APD}}}{Q}\sigma_V \approx \frac{d}{v_e}\frac{K\epsilon_0 A}{w}\frac{1}{G_{\text{APD}}G_{\text{amp}}N_{\text{min}}d_{\text{eff}}}\sigma_V \propto \frac{\sigma_V}{d} , \qquad (50)$$

under the (possibly naïve) assumption that $d \propto d_{\text{eff}} \propto w$.

As noted in Appendices A and B, the rise time Δ of the APD waveform is essentially the width of the avalanche current pulse, which is roughly d/v_e where d is the thickness of the depletion region (p-side) when the electric field is high enough ($> 10^4$ V/cm) that the electron drift velocity is saturated, with value $v_e = 0.1$ μm/ps. The value of d can be changed by changing the thickness of the p-side of the APD, so eq. (50) suggests that it is better if the p-side depletion region were thinner.

References

[1] F. Braun, *Ueber die Stromleitung durch Schwefelmetalle*, Ann. Phys. **229**, 556 (1874), http://physics.princeton.edu/~mcdonald/examples/detectors/braun_ap_229_556_74.pdf

[2] H.H.C. Dunwoody (Gen., US Army), *Wireless Telegraph System*, US Patent 837,616 (application filed Mar. 23, 1906), http://physics.princeton.edu/~mcdonald/examples/detectors/dunwoody_us837616_06.pdf

[3] G.W. Pierce, *Crystal Rectifiers for Electric Currents and Electric Oscillations*, Phys. Rev. **25**, 31 (1907), http://physics.princeton.edu/~mcdonald/examples/detectors/pierce_25_31_07.pdf

[4] W.H. Schottky, *Über den Austritt von Elektronern aus Glühdrähten bei verzörgernden Potentialen*, Ann. Phys. **349**, 1011 (1914), http://physics.princeton.edu/~mcdonald/examples/detectors/schottky_ap_349_1011_14.pdf *Über den Einfluss von Strukturwirkungen, besonders der Thomsonschen Bildkraft, auf die Elektronenemission der Metalle*, Phys. Z. **15**, 872 (1914), http://physics.princeton.edu/~mcdonald/examples/detectors/schottky_pz_15_872_14.pdf *Halbleitertheorie der Sperrschicht*, Naturw. **50**, 843 (1938), http://physics.princeton.edu/~mcdonald/examples/detectors/schottky_naturwissenschaften_52_843_38.pdf

[5] H.A. Bethe, *Theory of the boundary layer of crystal rectifiers*, MIT Rad. Lab. Rep. 43-12 (Nov. 23, 1942).

[6] A. Joffé, *Elastische Nachwirkung im kristallinischen Quarz*, Ann. Phys. **325**, 919 (1906), http://physics.princeton.edu/~mcdonald/examples/detectors/joffe_ap_325_919_06.pdf

[7] P.J. van Heerden, *The Crystal Counter*, dissertation, (Utrecht, 1946).

[8] K.G. McKay, *Electron Bombardment Conductivity in Diamond*, Phys. Rev. **74**, 1606 (1948), http://physics.princeton.edu/~mcdonald/examples/detectors/mckay_pr_74_1606_48.pdf

[9] R. Frerichs, *On the Relations between Crystal Counters and Crystal Phosphors*, J. Opt. Soc. Am. **40**, 219 (1950, http://physics.princeton.edu/~mcdonald/examples/detectors/frerichs_josa_40_219_50.pdf

[10] K.G. McKay, *Electron-Hole Production in Germanium by Alpha-Particles*, Phys. Rev. **84**, 829 (1951), http://physics.princeton.edu/~mcdonald/examples/detectors/mckay_pr_84_829_51.pdf

[11] W. Shockley, *The Theory of p-n Junctions in Semiconductors and p-n Junction Transistors*, Bell Syst. Tech. J. **28**, 435 (1949), http://physics.princeton.edu/~mcdonald/examples/detectors/shockley_bstj_28_435_49.pdf

[12] S. Ristić, A. Prijić and Z. Prijić, *Dependence of Static Dielectric Constant of Silicon on Resistivity at Room Temperature*, Serbian J. Elec. Eng. **1**, 237 (2004), http://physics.princeton.edu/~mcdonald/examples/detectors/ristic_sjee_1_237_04.pdf

[13] C. Canali *et al.*, *Electron and Hole Drift Velocity Measurements in Silicon and Their Empirical Relation to Electric Field and Temperature*, IEEE Trans. Electron Dev. **22**, 1045 (1975), http://physics.princeton.edu/~mcdonald/examples/detectors/canali_ieeeted_22_1045_75.pdf

[14] C. Jacobini *et al.*, *A Review of Some Charge Transport Properties of Silicon*, Solid State Elec. **20**, 77 (1977), http://physics.princeton.edu/~mcdonald/examples/detectors/jacoboni_sse_20_77_77.pdf

[15] M. McLish *et al.*, *A Reexamination of Deep Diffused Silicon Avalanche Photodiode Gain and Quantum Efficiency*, IEEE Trans. Nucl. Sci. **53**, 3049 (2006), http://physics.princeton.edu/~mcdonald/examples/detectors/mcclish_ieeetns_53_3049_06.pdf http://physics.princeton.edu/~mcdonald/LHC/KTM/concentration_profile2.xlsx

[16] R. Redus and R.Farrell, *Gain and noise in very high gain avalanche photodiodes: theory and experiment*, Proc. SPIE **2859**, 288 (1996), http://physics.princeton.edu/~mcdonald/examples/detectors/redus_spie_2859_288_96.pdf

[17] K.G. McKay and K.B. McAfee, *Electron Multiplication in Silicon and Germanium*, Phys. Rev. **91**, 1079 (1953), http://physics.princeton.edu/~mcdonald/examples/detectors/mckay_pr_91_1079_53.pdf

[18] R.J. McIntyre, *Multiplication Noise in Uniform Avalanche Diodes* , IEEE Trans. Elec. Dev. **13**, 164 (1966), http://physics.princeton.edu/~mcdonald/examples/detectors/mcintyre_ieeeted_13_164_66.pdf

[19] K.G. McKay, *Avalanche Breakdown in Silicon*, Phys. Rev. **94**, 877 (1954), http://physics.princeton.edu/~mcdonald/examples/detectors/mckay_pr_94_877_54.pdf

[20] S.L. Miller, *Avalanche Breakdown in Germanium*, Phys. Rev. **99**, 1234 (1955), http://physics.princeton.edu/~mcdonald/examples/detectors/miller_pr_99_1234_55.pdf

[21] C.A. Lee *et al.*, *Ionization Rates of Holes and Electrons in Silicon*, Phys. Rev. **134**, A761 (1964), http://physics.princeton.edu/~mcdonald/examples/detectors/lee_pr_134_A761_64.pdf

[22] R.J. McIntyre, *The Distribution of Gains in Uniformly Multiplying Avalanche Photodiodes: Theory*, IEEE Trans. Elec. Dev. **19**, 703 (1972), http://physics.princeton.edu/~mcdonald/examples/detectors/mcintyre_ieeeted_19_703_72.pdf

[23] R.J. McIntyre, *A New Look at Impact Ionization–Part I: A Theory of Gain, Noise, Breakdown Probability, and Frequency Response*, IEEE Trans. Elec. Dev. **46**, 1623 (1999), http://physics.princeton.edu/~mcdonald/examples/detectors/mcintyre_ieeeted_46_1623_99.pdf

[24] P. Yuan *et al.*, *A New Look at Impact Ionization–Part II: Gain and Noise in Short Avalanche Photodiodes*, IEEE Trans. Elec. Dev. **46**, 1632 (1999), http://physics.princeton.edu/~mcdonald/examples/detectors/yuan_ieeeted_46_1632_99.pdf

[25] G.J. Rees and J.P.R. David, *Nonlocal impact ionization and avalanche multiplication*, J. Phys. **43**, 243001 (2010), http://physics.princeton.edu/~mcdonald/examples/detectors/rees_jpd_43_243001_10.pdf

[26] A.G. Chynoweth, *Ionization Rates for Electrons and Holes in Silicon*, Phys. Rev. **109**, 1537 (1958), http://physics.princeton.edu/~mcdonald/examples/detectors/chynoweth_pr_109_1537_58.pdf